

# Convolutional Optical Encoders for Generalizable Image Compression

YUBO ZHANG<sup>1,\*</sup>, RUI CHEN<sup>3</sup>, ZHIHAO ZHOU<sup>1</sup>, AND ARKA MAJUMDAR<sup>1,5</sup>

<sup>1</sup>Electrical & Computer Engineering Department, University of Washington, Seattle, WA 98105, USA

<sup>3</sup>Massachusetts Institute of Technology, Cambridge, MA, USA

<sup>5</sup>Department of Physics, University of Washington, Seattle, WA 98105, USA

\* Yubo Zhang: yuboz4@uw.edu; Arka Majumdar: arka@uw.edu

Compiled February 23, 2026

**We investigate the utility of meta-optical encoders for generalizable image compression by leveraging their intrinsic shift-invariant point spread functions (PSFs). Compared with purely digital approaches, such optical encoders offer parallel and energy-efficient compression, enabling early data reduction prior to electronic processing and transmission, which is particularly attractive for resource-constrained and compact imaging systems. Although the operations realizable by a single passive optical layer remain fundamentally constrained, we systematically study several PSF encoding strategies combined with a total-variation (TV) digital reconstruction backend. Specifically, under identical compression ratios, we compare spatial binning, multi-channel random, and multi-channel orthogonal PSF based designs. Our results show that, at the same compression ratios, spatial binning achieves the highest reconstruction quality among all encoding strategies; however, it exhibits limited robustness to noise compared with multi-channel methods.**

<http://dx.doi.org/10.1364/ao.XX.XXXXXX>

## 1. INTRODUCTION

As an energy-efficient front-end for image compression[1, 2], meta-optical encoding offers the potential to reduce data volume at the point of acquisition, thereby easing subsequent data transmission and processing burdens, particularly for compact and resource (energy/latency)-constrained imaging systems. Incoherent imaging systems with meta-optical encoder can be well approximated by linear models, where the output intensity captured in the sensor is a weighted sum (determined by the position-dependent point spread function (PSF)) of the input intensity. This framework underlies a broad range of optical utilities such as functional imaging[3], computational spectrometers[4], and neural network front-ends[5]—where the

system performs a linear mapping between the object intensity and its measured intensity distribution. In many optical neural network and optical encryption[6] methods, approximated linear translational invariance plays a crucial role, allowing the imaging process to be well approximated as a convolution between the object intensity and an effective kernel (determined by the zero field-angle PSF of the optics).

Building upon this linear model, we simulate a meta-optical compressive encoding system coupled with a total variation (TV)-regularized digital reconstruction backend[7]. We chose to not employ a learned backend to ensure the generalizability of our imaging systems. Within a practical range of kernel sizes, we systematically sweep the kernel parameters and compare different kernel design strategies, evaluating their impact on image reconstruction quality under identical compression ratios.

We systematically compare several kernel design strategies—including a point PSF (1×1 normalized kernel) corresponding to ideal lens-based imaging (performing identical transformation during convolution), positive multi-channel random PSFs corresponding to multi-channel lensless imaging, signed multi-channel random kernels that introduce both positive and negative values, and orthogonal multi-channel kernels corresponding to a spatially multiplexed, single pixel imaging[8]-inspired design—where spatial binning is applied after each convolution to achieve compression—across two representative datasets, Celeba (containing face images)[9] and Arimp4 (a self-customized dataset derived from daily-activity videos from Project Aria)[10]. These two datasets are chosen to represent two different classes of images: in the first one (face), most pixels represent one object; whereas in the second (natural scenes), we have many different objects in the scene. All methods share the same scene-independent digital reconstruction backend, ensuring a fair comparison. Among these, spatial binning serves as baseline designs, while the orthogonal kernels employ a set of specially designed, mutually orthogonal kernels inspired by SPI principles to explicitly decorrelate the extracted features and improve reconstruction quality. By sweeping key hyperparameters, such as the kernel size, spatial binning ratio, TV regularization weight, and evaluating reconstruction performance across various noise levels and compression ratios, we develop a comprehensive framework for understanding how different kernel design strategies affect reconstruction fidelity

and noise robustness.

One particularly notable observation is that, at the same compression ratio, compression based solely on a lens PSF consistently exhibits strong reconstruction fidelity, in some cases even outperforming the orthogonal kernel designs. From a frequency-domain perspective, this behavior can be attributed to the lens PSF's ability to preserve a larger portion of the object's spatial frequency content, as reflected by its more favorable modulation transfer function (MTF)[11]. In contrast, while orthogonal kernels effectively decorrelate measurements, they do not necessarily maximize spatial frequency preservation under the same optical constraints. At the same time, we observe that multichannel kernel designs improve noise resilience, especially under low signal-to-noise ratio conditions. By distributing information across multiple measurement channels, multichannel encoders reduce the sensitivity of reconstruction to noise and measurement perturbations, highlighting an important trade-off between frequency preservation and robustness.

These observations motivate a deeper examination of the fundamental limitations of convolution-based optical encoders. Before integrating such optical convolutional front-ends with more sophisticated digital backends, it is essential to identify the true information bottlenecks imposed by the optical kernel itself. Our comparative study therefore provides an overview of the design space of convolutional meta-optical encoders, offering physical and computational insights that inform the exploration of alternative optical layer architectures beyond convolution.

## 2. DESIGN AND RESULTS

An overview of the proposed workflow is shown in Fig. 1. Image compression and reconstruction experiments are conducted on two representative datasets, CelebA and Arimp4, representing relatively simple and more complex data, respectively, to verify the consistency of observed trends across different data complexities. After the optical convolution layer, the encoded measurements are spatially downsampled to emulate the compression and sampling process of a practical image sensor. The original image is then reconstructed using a linear regression model with total variation (TV) regularization, which serves as a simple and interpretable digital backend for evaluating the impact of different optical encoding strategies.

The size of the convolution kernel  $m$  is swept from 0 to 19. For larger kernels, a correspondingly higher spatial downsampling (via average pooling) rate is applied to achieve different compression ratios, defined as the ratio between the dimensionality of the ground-truth image and that of the compressed measurement. Figure 2 shows the reconstruction visual information fidelity (VIF, which quantifies how much visual information from a reference image is preserved in a distorted image based on information theory and natural scene statistics) as a function of compression ratio (CR) for the four encoding strategies considered. Error bars indicate the standard deviation across 5 random seeds for the random-kernel-based methods.

The encoding strategies (with different kernels) are as follows:

1. Lens Imaging & Spatial Binning (average pooling). The image is directly average-pooled using an  $m$  by  $m$  kernel, equivalent to spatial binning of the original image with a stride of  $(m, m)$ .
2. Multi-channel positive random PSFs. A multi-channel random convolution with  $n_{\text{channel}} = 5$  where each channel employs an independent non-negative random kernel of size  $m$

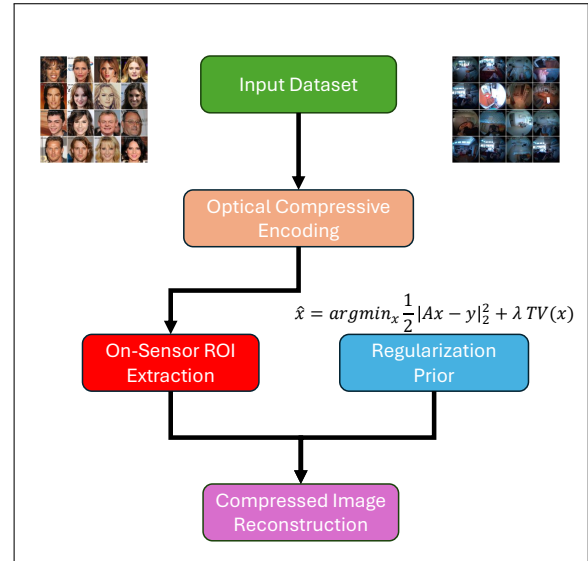


**Fig. 1.** Schematic of our workflow for image compression, where the convolution encoding is performed by meta-optics. We apply average binning as region of interest (ROI) detection to compress the image after convolution. Linear regression with total variation (TV) regularization is used to reconstruct the image.

by  $m$ . The kernel intensities are normalized to represent PSFs. After convolution, each channel output is spatially binned with a stride of  $(m, m)$ .

3. Multi-channel signed random kernels. Similar to the positive random case, except that the random kernels contain both positive and negative values. All other settings, including kernel size, channel count, and spatial binning, remain the same.

4. Multi-channel orthogonal kernels. A multi-channel kernel design with mutually orthogonal kernels of size  $(m, m)$ , where kernels across channels are mutually orthogonal. The kernels are constructed by progressively incorporating spatial frequency components, from low-frequency modes to higher-frequency Fourier basis functions along the horizontal and vertical directions. Each channel output is subsequently binned with a stride of  $(m, m)$  to maintain a consistent compression ratio.

For all multi-channel strategies, the compression ratio is calculated based on the total dimensionality of the sensed measurements aggregated across all channels.

From the results shown in Fig. 2, we observe that the VIF curves of TV reconstruction exhibit highly consistent trends across the two datasets, despite their different levels of complexity. This consistency motivates us to report only the results on the Arimp4 dataset in the subsequent analysis. Notably, at the same compression ratio, the binning strategy achieves the highest reconstruction VIF, whereas introducing negative values into the PSF leads to degraded and unstable reconstruction performance.

This behavior can be understood from a spatial frequency-domain perspective. In the case of imaging and binning, the optical layer effectively implements an identity transformation followed by spatial downsampling, whose corresponding convolution kernel (a  $1 \times 1$  kernel) yields a full modulation transfer function (MTF) of the system, which means that all frequency components of the input image are preserved. In contrast, introducing negative values into the PSF redistributes the cap-

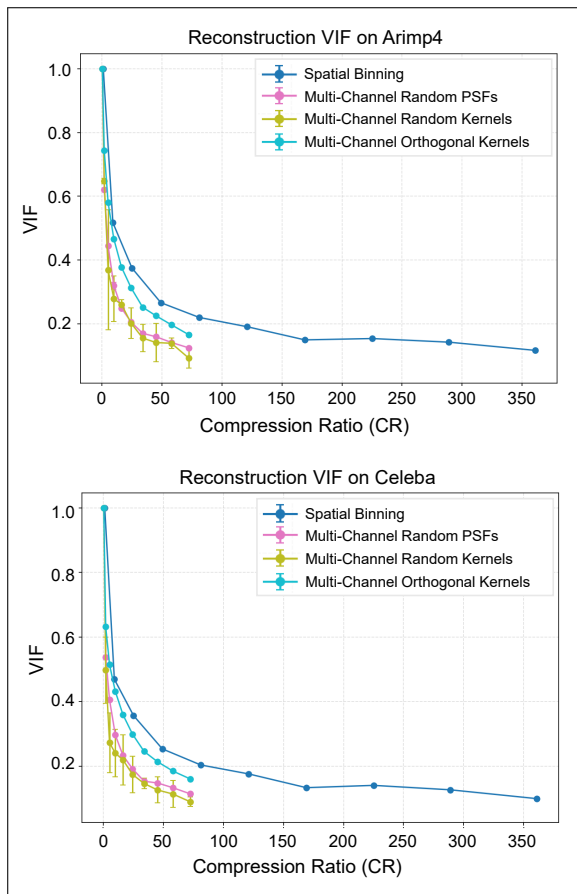


**Fig. 2.** Reconstruction VIF (Visual Information Fidelity) vs Compression Ratio on Arimp4 (up) and Celeba (down) dataset with different kernel design strategies.

tured information towards higher spatial frequencies, resulting in reduced low-frequency preservation in the MTF. The loss of low-frequency information, which carries most of the image energy and structural content, consequently leads to inferior reconstruction performance.

For multichannel encoders, the orthogonal kernel design is more efficient than multichannel random strategies, as its kernels progressively extract information from low to high spatial frequencies. However, at the same overall compression ratio, its reconstruction VIF remains lower than that of spatial binning, since the inclusion of high-frequency kernels reduces the average channel efficiency under strong compression. Nevertheless, this behavior highlights spatial or time-division multiplexing—particularly orthogonal encoding as a powerful mechanism for improving reconstruction performance under fixed sensor size constraints.

On the Arimp4 dataset, we further sweep the TV regularization parameter  $\lambda$  in the reconstruction formulation.

$$\hat{x} = \min_x \|Ax - b\|_{l_2} + \lambda \text{TV}(x)$$

As shown in Fig. 3, among the values tested,  $\lambda = 10^{-1}$  consistently delivers the best reconstruction performance. This observation indicates that the Arimp4 dataset is best matched by a TV prior to this strength, and therefore we adopted this value in subsequent experiments.

From the evolution of the reconstruction curves, we observe a clear transition in the dominant loss term. For  $\lambda < 10^{-1}$ , the data fidelity term dominates the optimization, and increasing  $\lambda$  improves the reconstruction VIF across all strategies by suppressing noise and mitigating ill-conditioning. Around  $\lambda = 10^{-1}$ , an optimal balance is achieved between the data fidelity term and the TV regularization, resulting in the highest reconstruction quality. As  $\lambda$  increases beyond this point, the TV term becomes dominant, enforcing overly strong smoothness priors that over-smooth the reconstructed images and consequently degrade the VIF.

Across the explored range of  $\lambda$ , the reconstruction VIF curves of all strategies exhibit a nearly identical ranking trend. In most cases, spatial binning consistently achieves the highest performance and remains the leading approach. At the optimal regularization strength of  $\lambda = 10^{-1}$ , the orthogonal multi-channel strategy attains a performance level comparable to that of binning. At  $\lambda = 10^1$ , however, the overly aggressive TV prior disrupts the numerical balance between the data fidelity and regularization terms, leading to a non-monotonic dependence of VIF on the compression ratio across all strategies. When  $\lambda$  is further increased to  $10^3$ , the reconstruction quality degrades more severely overall; however, spatial binning again achieves the highest VIF, and the VIF curves revert to the monotonic decreasing trend with increasing compression ratio observed at smaller values of  $\lambda$ .

Finally, we compare the noise robustness of three representative strategies. The signed random kernel design is excluded from this comparison due to its consistently inferior performance and higher computational cost in simulation. The comparison is conducted under a fixed compression ratio of  $\text{CR} = 4$ , as shown in Fig. 4. For each SNR level, the reported reconstruction metrics are obtained by averaging over multiple independent samplings of Poisson noise.

At high SNR, spatial binning strategy converges to better reconstruction fidelity than two multichannel strategies at the same compression ratio. This behavior is consistent with their stronger preservation of low-frequency information under low-noise conditions. However, as the noise level increases (i.e., SNR decreases), the single channel spatial binning method suffers more severely from noise, leading to a faster degradation in reconstruction quality. In contrast, multichannel strategies exhibit better noise resilience, benefiting from information diversity and aggregating measurements across multiple measurement channels.

This observation highlights an inherent trade-off between reconstruction fidelity in low-noise regimes and robustness under noisy acquisition, emphasizing the role of multi-channel encoding in mitigating noise-induced performance degradation under fixed sensor and compression constraints. This trade-off is consistent with the design intuition of single-pixel imaging, where multiple complementary measurements are leveraged to improve robustness to noise at the expense of per-measurement efficiency.

### 3. SUMMARY

In summary, we present a systematic study of convolution-based meta-optical encoders for compressive imaging under simulated sensor and noise constraints. By comparing a range of physically motivated PSF designs within a unified digital reconstruction framework, we show that simple and interpretable encoders such as lens imaging with binning can achieve strong

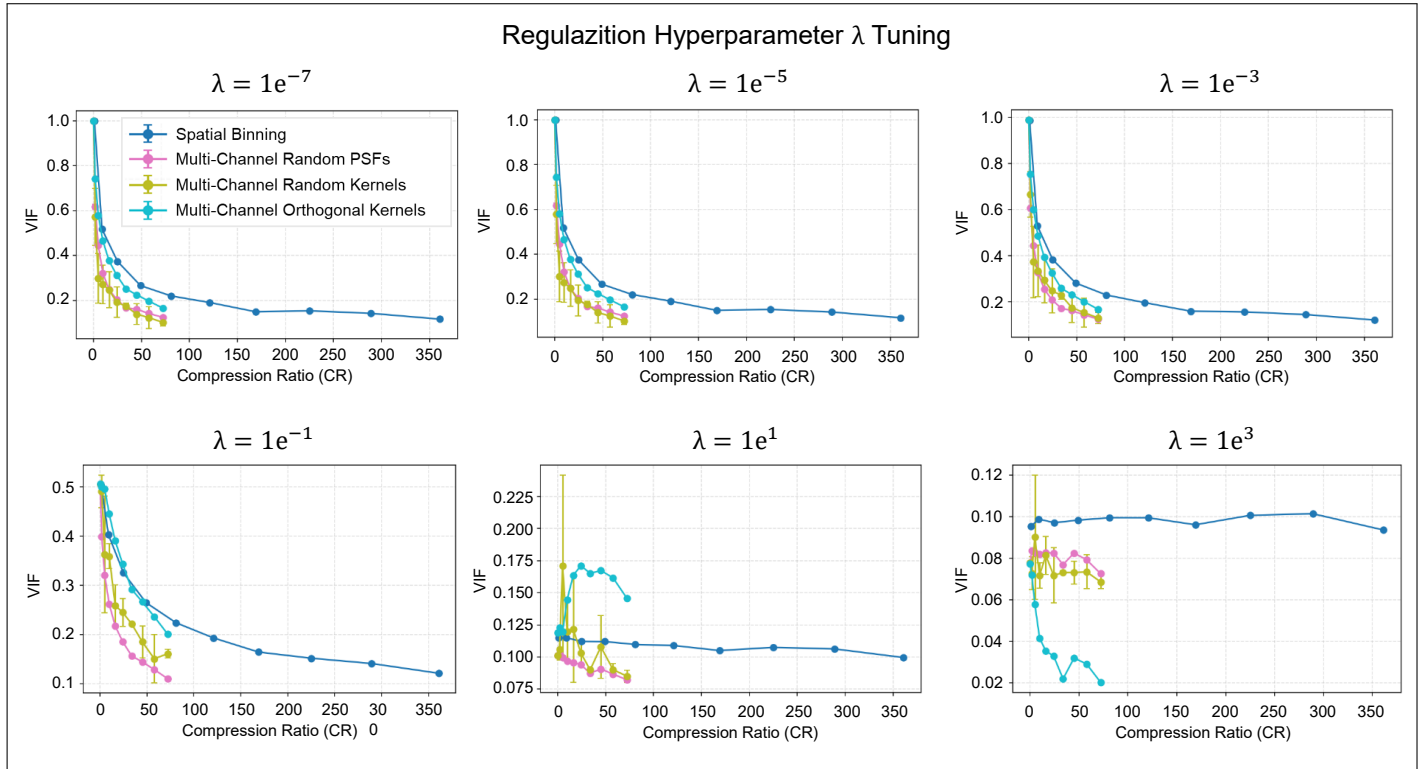


**Fig. 3.** Reconstruction VIF on TV regularization hyperparameter  $\lambda$  ranging from  $10^{-7}$  to  $10^3$ . Larger values of  $\lambda$  impose a stronger prior favoring piecewise-smooth images with smoother backgrounds. All results in this sweep are obtained on the Arimp4 dataset.

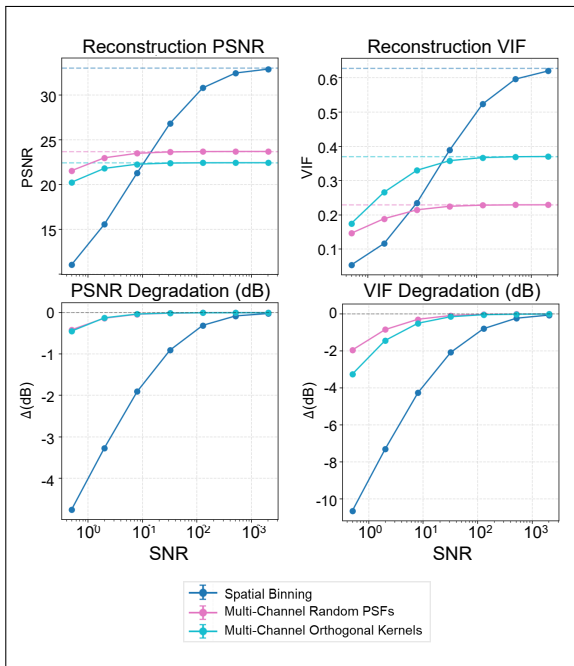


**Fig. 4.** Comparison of reconstruction quality across varying SNRs between 4 strategies. The left column shows PSNR and its corresponding dB-scale loss, while the right column shows VIF and its corresponding dB-scale loss.

reconstruction fidelity at fixed compression ratios due to their effective preservation of low-frequency information. In contrast,

multi-channel and orthogonal encoding strategies exhibit improved noise robustness through spatial multiplexing, revealing a fundamental trade-off between frequency preservation and noise resilience.

More broadly, our results clarify the role of optical encoders in image compression pipelines. Unlike learned image compression models, where nonlinear representation learning is central, optical encoders are inherently limited to linear, intensity-domain operations dictated by physics. Consequently, the key design bottleneck lies not in feature decorrelation, but in how spatial frequency content is preserved or discarded by the optical kernel. Our findings indicate that, within this constrained design space, interpretability and frequency-domain behavior of the PSF are more critical than aggressive decorrelation strategies.

From this perspective, convolution-based optical encoders should be viewed not as replacements for digital learned image compression encoders, but as physically grounded front-ends that reshape information prior to digital processing. Identifying the information bottleneck imposed by the optical layer is therefore essential for effective integration with learned reconstruction or entropy-coding backends. We anticipate that these insights will inform the co-design of future optical-digital compression systems, where interpretable optical encoders complement data-driven learned models.

Code implementation of this work can be found at: [GitHub repository](#).

#### 4. ACKNOWLEDGEMENT

#### REFERENCES

1. Y. Shechtman, Y. C. Eldar, A. Szameit, and M. Segev, *Opt. express* **19**, 14807 (2011).

2. Y. Zhang, R. Chen, M. Choi, *et al.*, "General image compression using random-psf metasurfaces and computational back-end," in *2024 Conference on Lasers and Electro-Optics (CLEO)*, (IEEE, 2024), pp. 1–3.
3. N. Antipa, G. Kuo, R. Heckel, *et al.*, *Optica* **5**, 1 (2017).
4. D.-g. Lee, G. Song, C. Lee, *et al.*, *Sci. Adv.* **11**, eadv2376 (2025).
5. J. Xiang, M. Choi, Y. Zhang, *et al.*, arXiv preprint arXiv:2508.08421 (2025).
6. R. Audhkhasi and M. L. Povinelli, *Sci. reports* **11**, 22669 (2021).
7. Z. Shen, Z. Geng, and J. Yang, *Stat. Optim. & Inf. Comput.* **3**, 1 (2015).
8. G. M. Gibson, S. D. Johnson, and M. J. Padgett, *Opt. express* **28**, 28190 (2020).
9. T. Karras, T. Aila, S. Laine, and J. Lehtinen, *CoRR* **abs/1710.10196** (2017).
10. Z. Lv, N. Charron, P. Moulon, *et al.*, arXiv preprint arXiv:2402.13349 (2024).
11. Y. Zhang, J. Fröch, J. Xiang, *et al.*, arXiv preprint arXiv:2512.08109 (2025).